Computational Materials Science 100 (2015) 21–30

Contents lists available at ScienceDirect

Computational Materials Science

journal homepage: www.elsevier.com/locate/commatsci

Analysis of iron powder design for compaction process

Jae Hoon Jeong [a], Seung Kyu Ryu [b], Seong Jin Park [a,*], Hong Chul Shin [c], Ji-Hun Yu [d]

[a] Department of Mechanical Engineering, Pohang University of Science and Technology, Republic of Korea
[b] Department of Advanced Nuclear Engineering, Pohang University of Science and Technology, Republic of Korea
[c] Advanced Metallic Materials Research, Research Institute of Industrial Science and Technology, Republic of Korea
[d] Powder & Ceramics, Korea Institute of Materials Science, Republic of Korea

ARTICLE INFO

Article history:
Received 29 August 2014
Received in revised form 13 November 2014
Accepted 16 November 2014
Available online 11 December 2014

Keywords:
Powder compaction
Powder design parameters
Material properties
Final properties
Sensitivity analysis
Regression model

ABSTRACT

This paper aims at finding a relationship among the iron powder design parameters, the material properties, and the final properties. The iron powder design parameters were the composition of graphite, particle size, and the composition of lubricant. The material properties in Shima–Oyane constitutive model are α, β, γ, a, b, and n. The final properties of green bodies are green density, density deviation, effective stress, hydrostatic pressure, effective strain, and volumetric strain. The correlations between the powder design parameters and the material properties were obtained by compaction experiments with regression method. The correlations between the material properties and the final properties were obtained by the compaction simulation with regression method. The regression model which shows the correlations between the powder design parameters and the final properties with the fixed process conditions and geometry were developed. This regression model gives the generic information of the powder design.

1. Introduction

The numerical simulation of powder compaction was widely used in the powder metallurgy field. The whole schematic diagram of the compaction simulation is shown in Fig. 1. The process conditions, geometries, and material properties of powder determine the final properties of green bodies. The powder design parameters determine the material properties of powder. Therefore, the powder design parameters such as the composition of graphite, particle size, and the composition of lubricant affect the final properties of green bodies in iron–carbon powder compaction [1].

The simulation was usually used to optimize process conditions and geometries with the fixed material properties [2,3]. The simulation can be used to determine the powder design parameters with the fixed process conditions and geometries, once the correlation between the powder design parameters and the material properties is found. The commercial software, PMSOLVER was used in this study and the simulation tool was verified in the previous study [4].

The powder design parameters, material properties, and the final properties are summarized in Table 1 with their notations in this paper. The tap density and green density represent the relative value compared to the full density. The density deviation represents the difference between maximum relative density and minimum relative density.

The Shima–Oyane yield model was employed for compaction simulation. The general form of Shima–Oyane constitutive model was expressed in Eq. (1) [4,5].

$$\Phi = (\sigma_{Effect}/\sigma_f)^2 + \alpha(1-\rho)^{\beta}(\sigma_{Hydro}/\sigma_f)^2 - \rho^{\gamma} \quad (1)$$

Φ is the yield surface of the porous materials. α, β, and γ are the material properties. σ_{Hydro} and σ_{Effect} are the hydrostatic pressure and the effective stress, respectively. ρ is the relative density. σ_f is the flow stress of the matrix materials and it can be expressed as a rigid and strain hardening model in Eq. (2) [6].

$$\sigma_f = a + b\varepsilon_{Effect}^{n} \quad (2)$$

ε_{Effect} is the effective strain of the matrix material. a, b, and n are the material properties which can be also determined from the compressibility curve.

Drucker–Prager failure model was employed to predict cracking formulation [7]. The equation of the failure surface was expressed as Eq. (3).

$$F_s = \sigma_{Effect} - \sigma_{Hydro}\tan\beta - d \quad (3)$$

β is the cohesion angle and d is the cohesive strength. These are the functions of relative density. $\tan\beta$ and d were set as constant values of $\tan\beta = 3.41$ and $d = 0.01$ MPa in the previous study [4]. The crack

* Corresponding author.
E-mail address: sjpark87@postech.ac.kr (S.J. Park).

http://dx.doi.org/10.1016/j.commatsci.2014.11.028
0927-0256/

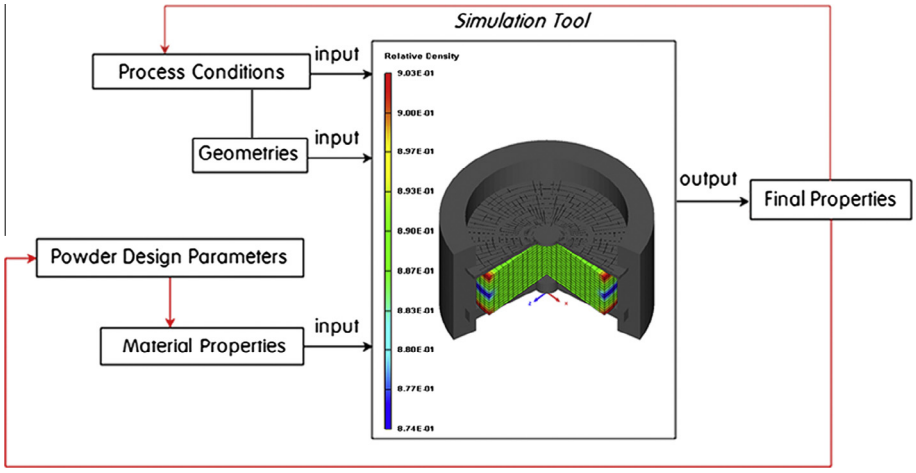

Fig. 1. Schematic diagram of compaction simulation.

Table 1
The notations of powder design parameters, material properties, and the final properties.

Powder design parameters	Notation	Material properties	Notation	Final properties	Notation
Composition of graphite (wt.%)	G	Tap density	ρ_{Tap}	Green density	ρ_{Green}
Particle size (μm)	P	γ	γ	Density deviation	$\Delta\rho$
Composition of lubricant (wt.%)	L	a (MPa)	a	Effective stress (MPa)	σ_{Effect}
		b (MPa)	b	Hydrostatic pressure (MPa)	σ_{Hydro}
		n	n	Effective strain	ε_{Effect}
				Volumetric strain	ε_{Vol}

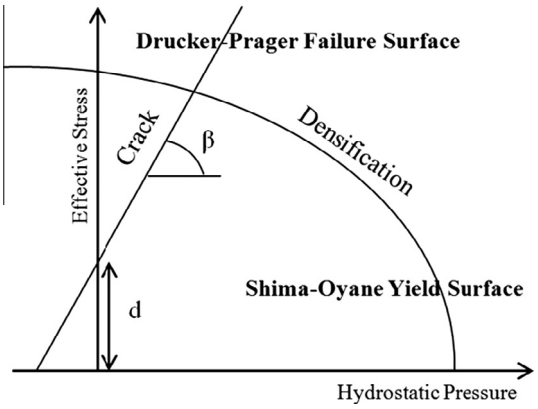

Fig. 2. Shima–Oyane yield model and Drucker–Prager failure model.

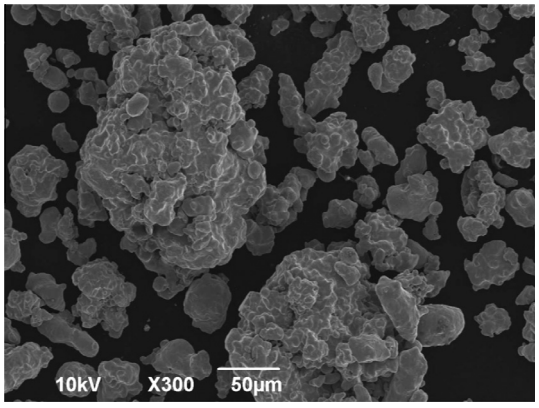

Fig. 3. Morphology of A1000 iron powder.

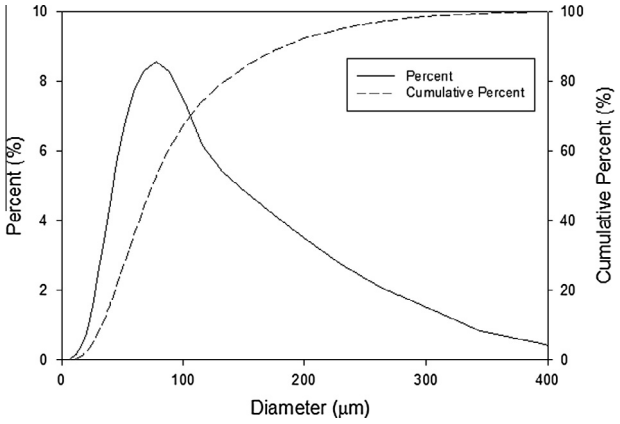

Fig. 4. Particle size distribution of A1000 iron powder.

can be occurred above Drucker–Prager failure surface and the densification can be occurred above Shima–Oyane yield surface as shown in Fig. 2.

2. Experimental procedure

2.1. Materials

A1000 iron powder fabricated by the water atomization was used in this study. The pycnometer density was 7.88 g/cm^3 and tap density was 0.47. The morphology of this powder is shown in Fig. 3. The particles have the irregular shape and the particle sizes are various. The particle size distribution was measured by the laser scattering particle size distribution analyzer (LA-95V2). D_{10},